Neutron-proton equilibration in dynamically deformed systems at E=15, 25, 35 and 45 MeV/nucleon

A. Jedele, A.B. McIntosh, J. Gauthier, L. Heilborn, A. Rodriguez Manso, A. Zarrella, and S.J. Yennello

Recent work [1,2] has shown NZ equilibration follows first-order kinetics within excited projectile-like fragments (PLF*) in ^{70}Zn, ^{64}Zn and ^{64}Ni reaction systems at 35MeV/nucleon. Future experiments have been proposed to examine the characteristics of NZ equilibration in ^{40}Ca+^{64,70}Zn at 15A, 25A, 35A and 45MeV/nucleon with the NIMROD array [3].

Constrained Molecular Dynamics (CoMD) [4] simulations were performed for ^{40}Ca+^{64,70}Zn reaction systems at 45MeV/nucleon and the ^{40}Ca+ ^{64}Zn reaction system at 35MeV/nucleon. For each reaction system 10,000 events were analyzed and fragments were sorted based on atomic number and velocity. The heaviest fragment (HF) from the excited projectile-like fragment was required to have a HF>6 and a velocity greater than 0.12c (~30% of v_{beam} for 45 MeV/nucleon systems). For the second heaviest fragment (LF), LF>3 and v_L>0.08c. The velocity requirement was to ensure fragments are

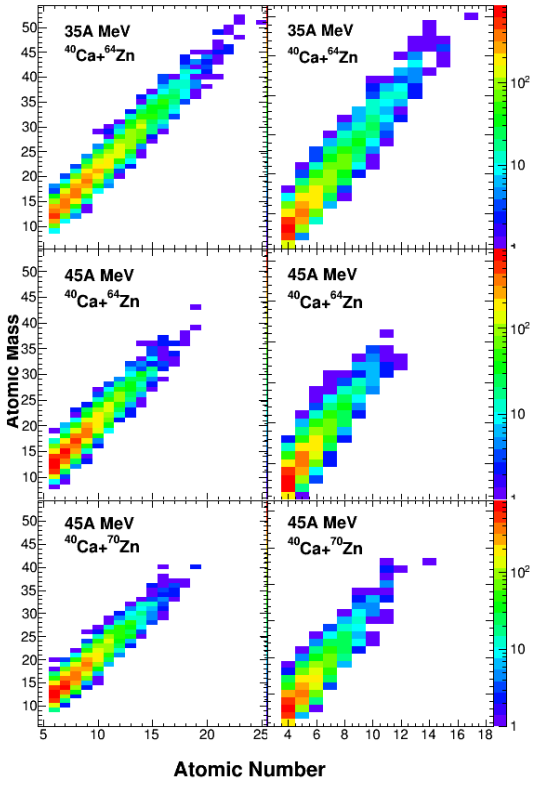

FIG. 1. The mass number vs. atomic number of the HF (left) and LF (right) for the three reaction systems. The ^{40}Ca+^{64}Zn at 35 MeV/nucleon is on the top row; ^{40}Ca+^{64}Zn at 45 MeV/nucleon in the middle and ^{40}Ca+^{70}Zn at 45 MeV/nucleon in the bottom. For all 6 distributions, the greatest yield is seen at low Z (Z=7 for HF and Z=4 for LF). The 35 MeV/ nucleon system has a greater atomic number and mass number distribution.

primarily originating from the PLF*. Approximately 5% of events passed the above cuts for all three reaction systems. The mass number versus the atomic number for both fragments and all reaction systems is shown in Fig. 1. The largest yield is shown at low Z, especially for the higher energy systems. The lower energy system has a greater range in atomic number for both HF and LF. The multiplicity distribution for all fragments including those originating from the TLF* ranges from 10-70 and is peaked at 55 for the 45MeV/nucleon systems. For the 35MeV/nucleon system, the multiplicity distribution ranges from 10-60 and is peaked at 45.

For detector design, the angular distribution and energy as a function of angle were considered. The energy as a function of angle is shown in Fig. 2. For both HF and LF, the energy is centered significantly lower than beam energy. The angular distributions for both the 35 and 45 MeV/nucleon reaction systems are very similar. The lab angles ranges from 0-40° for HF and 0-60° for LF. The vast majority of particles were located below 20° for HF and below 40° for LF. Based on the angular distribution, rings 2-9 (3.6-45.0°) in NIMROD will be of highest priority. Looking at the energy, the majority of HF is located between 100-600 MeV for 45 MeV/nucleon. The majority of HF for 35 MeV/nucleon is lower at 100-500 MeV. For both energies, there are particles with much greater energies, above 1200 MeV for 45 MeV/nucleon and above 1000 MeV for 35 MeV/nucleon. The majority of the LF distribution is lower between 25-250 MeV and extends up to approximately 600 MeV for 45 MeV/nucleon. For 35 MeV/nucleon, the majority of LF is lower energy at 25-200 MeV and the distribution goes as high as approximately 600 MeV.

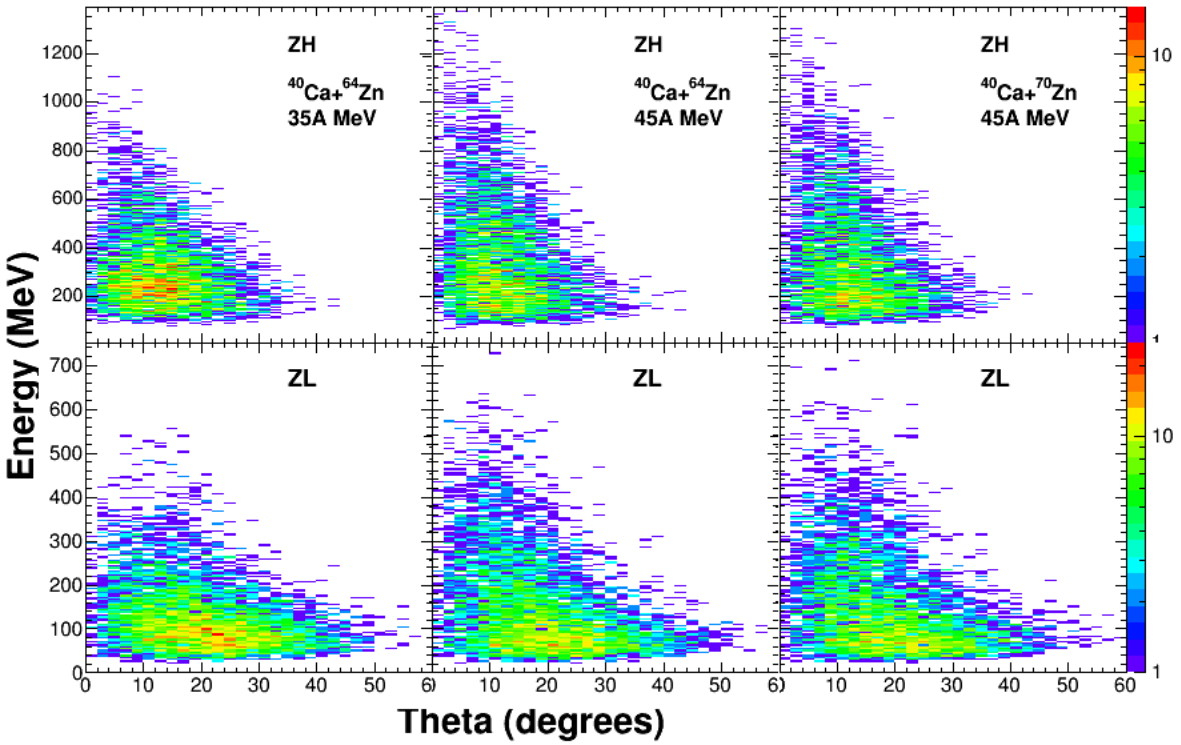

FIG. 2. Energy vs. theta. The top row corresponds to HF; bottom to LF. For HF, the energy distribution ranges from 100-600 MeV for 45 MeV/nucleon and 100-500 MeV for 35 MeV/nucleon. The angular distribution is between 0-40°. The energy distribution for LF ranges from 25-250 MeV for 45 MeV/nucleon and is slightly lower at 25-200 MeV for 35 MeV/nucleon. The angular distribution is between 0-60°.

Energy loss calculations were performed. CycSrim was used to calculate the energy loss in the target, a Si1, Si2 and CsI. The thickness of the Si2 was 500 μm and the thickness of the CsI was 6.0 cm (thinnest CsI in NIMROD). Two different Si thicknesses were tested for the front Si (100 μm and 150 μm). Results showed most particles were detected in either the ΔE-E or E-CsI/ΔE-CsI. For LF, 17-29% stopped in the ΔE and approximately 5-20% of HF stopped in the ΔE. The ΔE-E and E-CsI for HF and LF are shown in the middle and right part of Fig. 3. The left-hand side of Figure 3 is the ΔE vs. Z for all fragments stopping in the 1st Si.

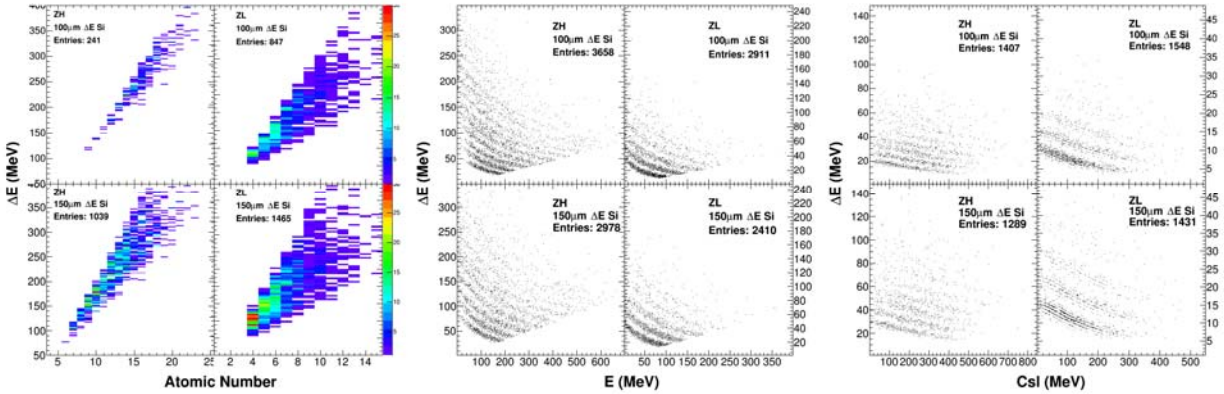

FIG. 3. From left to right: ΔE vs. Atomic number for fragments that stopped in the 1st Si, ΔE vs. E, and ΔE vs. CsI for 35 MeV/nucleon. For each 4 panel, the top row corresponds to the 100 μm 1st Si. The bottom row has a 1st Si thickness of 150 μm. The HF is on the left-hand side and LF is on the right. The number of events per identification method is shown in the upper right-hand side of each panel. Most of the fragments are identified with the 1st and 2nd Si detector.

Future work will focus on examining the equilibration between $^{48}Ca+^{64,70}Zn$ at 15A, 25A, 35A and 45A using COMD simulations. Results will help further determine which rings of NIMROD will be needed for the experiment. NIMROD will be outfitted with more supertelescopes in strategic locations to improve the chances of measuring with isotopic resolution the two heaviest daughters of the PLF*.

[1] A. Jedele, *et al*. Phys. Rev. Lett **118**, 062501 (2017).

[2] A. Rodriguez Manso, *et al*. Phys. Rev. C **95**, 044604 (2017).

[3] S. Wuenschel, *et al*. Nucl. Intrum. Methods Phys. Res. **A604**, 578 (2009).

[4] M. Papa, T. Maruyama, and A. Bonasera, Phys. Rev. C **64**, 024612 (2001).